

DEFORMABLE SURFACE REGISTRATION FOR BREAST TUMORS TRACKING: A PHANTOM STUDY

Bogdan Mihai Maris
Altair Robotics Laboratory
Department of Computer Science
University of Verona
Verona, Italy
email: bogdan.maris@univr.it

Paolo Fiorini
Altair Robotics Laboratory
Department of Computer Science
University of Verona
Verona, Italy
email: paolo.fiorini@univr.it

ABSTRACT

A phantom study for breast tumor registration based on the deformation of the external surface is proposed. This study aims at the integration into an image guided system for breast cancer biopsy or ablation. To compensate potentially large breast displacements, due to different positions of the breast during biopsy or ablation compared with pre-operative data, where the diagnosis was made, an initial linear alignment using visible landmarks is involved, followed by thin-plate spline (TPS) registration of the linearly aligned surfaces. Subsequently, the TPS deformation will be applied to the tumors. The results were validated using a multimodal phantom of the breast, while the tumors and the surface were segmented on four different positions of the phantom: prone, supine, vertical and on a side. The use of computed tomography (CT) dataset allowed us to obtain a very precise segmentation of the external surface, of the tumors and the landmarks. Despite large variation among the different positions of the phantom due to the gravitational force, the accuracy of the method at the target point was under 5 millimeters. These results allow us to conclude that, using our prototype image registration system, we are able to align acquisition of the breast in different positions with clinically relevant accuracy.

KEY WORDS

Computed tomography, image registration, image-guided interventions, multimodal imaging, diagnostic devices.

1 Introduction

Breast cancer is the most frequently diagnosed cancer and the leading cause of cancer death in women worldwide. The diagnosis of the breast cancer is driven by mammography and preoperative magnetic resonance images (MRI) in which the patient is standing or lying prone with pendant breasts, while the biopsy is performed with the patient in supine or semi-vertical position for the ultrasound (US) guided procedure or prone, when the procedure is done in the MRI room. The breast will undergo significant shape change between the pre-biopsy or preoperative phase and the biopsy or intraoperative phase, even when the acquisitions are performed in similar positions, causing the tumor

to deform and change location. The intraoperative imaging systems have less resolution than the preoperative ones (e.g. intraoperative MRI) and 50% of the non palpable tumors are not visible by US [17].

In this context, the registration of the preoperative data to the patient underlying the biopsy could improve the precision of the procedure. The breast is a highly deformable structure, therefore there is a high interest in modeling these deformations to capture the transformation of the breast between different imaging acquisitions. Some of these methods were focused on biomechanical modeling and how these approximate methods can be employed to create non-rigid registration methods to solve for image registration and, in case of the integration into an image guided interventional tool, for the correspondence between the images and the physical space of the intervention.

The accuracy of the biomechanical approach fails to meet clinically acceptable levels of computational cost and time, and the complexity of applying patient-specific biomechanical modelling to routine clinical practice.

Another line of research in image registration is based on the minimization of a measure of dissimilarity between the two (or more) images to be registered. The measures of dissimilarity range from sum of square differences and cross correlation in the case of mono-modal registration to mutual information in case of multi-modal images. One of the first clinical works for 3-D registration of the breast using normalized mutual information and free-form deformation derived from B-spline function was presented by [18].

An exhaustive review in the field of breast biomechanical modelling can be found in [10], while [4] reviews current developments in breast image registration techniques, and comments on their clinical relevance, individual capabilities, and open challenges. Some of the main drawbacks of the intensity based approaches, if used in image guided procedures, are the computation time, the optimization process that finds only local minimum, the distance measures that are very sensitive to noise and incomplete domains [12].

Image guided breast biopsy is a challenging task and the registration in this context has received little attention. Preliminary results that employed the biomechanical ap-



Figure 1. Breast phantom in horizontal or supine (left) and vertical (right) positions.

proach were presented by [6], while MRI and US approach was used by [7]. An image guided breast surgery system using supine MRI images, biomechanical modeling, rigid and nonrigid registration was presented by [8]. In [16] the authors introduced a hybrid breast biopsy system that solves the registration between MRI and US data by constraining the breast into an apparatus that is compatible with the MRI acquisition scanner and allows the connection of an US probe.

Under these circumstances, we propose here an approach that implements thin-plate spline (TPS) interpolation of the breast surface to ensure consistency of the deformation and to compute the closed form solution of the registration transformation that is subsequently applied to the tumors, which represent the target of the biopsy procedure. The TPS [5] have been already used to model the breast deformation during mammography for MRI to x-Ray fusion [2]. The work presented in [15] uses the TPS spline interpolation as a gold standard reference in breast surface non-rigid registration, in order to verify the results obtained using a biomechanical model of the breast.

2 Image acquisition and processing

The images used in this study were acquired from a multi-modality breast phantom CIRS 073¹ placed in four different positions: prone, supine, vertical and on a side (see Figure 1). The phantom accurately mimics the heterogeneous appearance of breast tissue under ultrasound, mammography, MRI, and CT, and has cystic and dense lesions embedded within the breast background. Half of the dense lesions are spherical and have a 100-300 micron microcalcification embedded within it, while the other half have a spiculated shape similar with the shape of the suspicious masses in breast cancer. The phantom includes a flexible membrane that simulates the look and feel of skin during scanning and

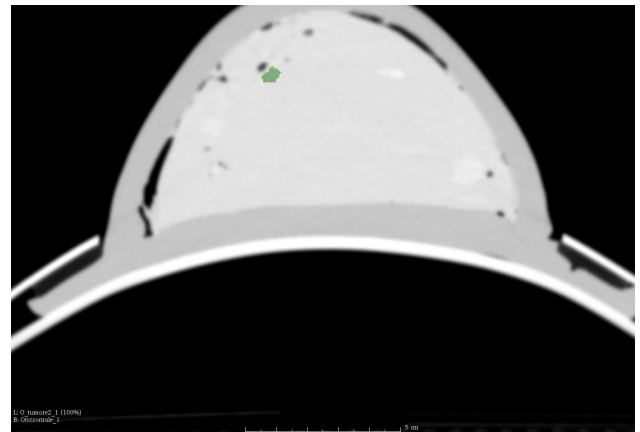


Figure 2. CT scan of the breast phantom. There are some artificial lesions visible and one of the lesions is segmented (green area).

biopsy. The skin material closes up on itself when punctured with a needle. The material inside the phantom is formulated to minimize the effect of needle tracks while practicing biopsy techniques on the embedded masses.

High resolution CT images were acquired with a Philips Brilliance 6 scanner and a reconstructed voxel size of $0.58 \times 0.58 \times 1 \text{ mm}^3$, while the slice resolution in plane was of 512×512 pixels (Figure 2).

A schematic overview of the structure of the processing pipeline is given in Figure 3. The use of the phantom is motivated by different factors: incipient stage of the work, to establish a ground truth for the result, to test the complete setup performance in term of both accuracy and time consumption. We can assess the ground truth since the only uncertainty in the setup is given by the accuracy of the acquisition and of the segmentation.

For each position of the breast, we have segmented the external surface using Insight Registration and Segmen-

¹Computerized Imaging Reference Systems, Inc., USA

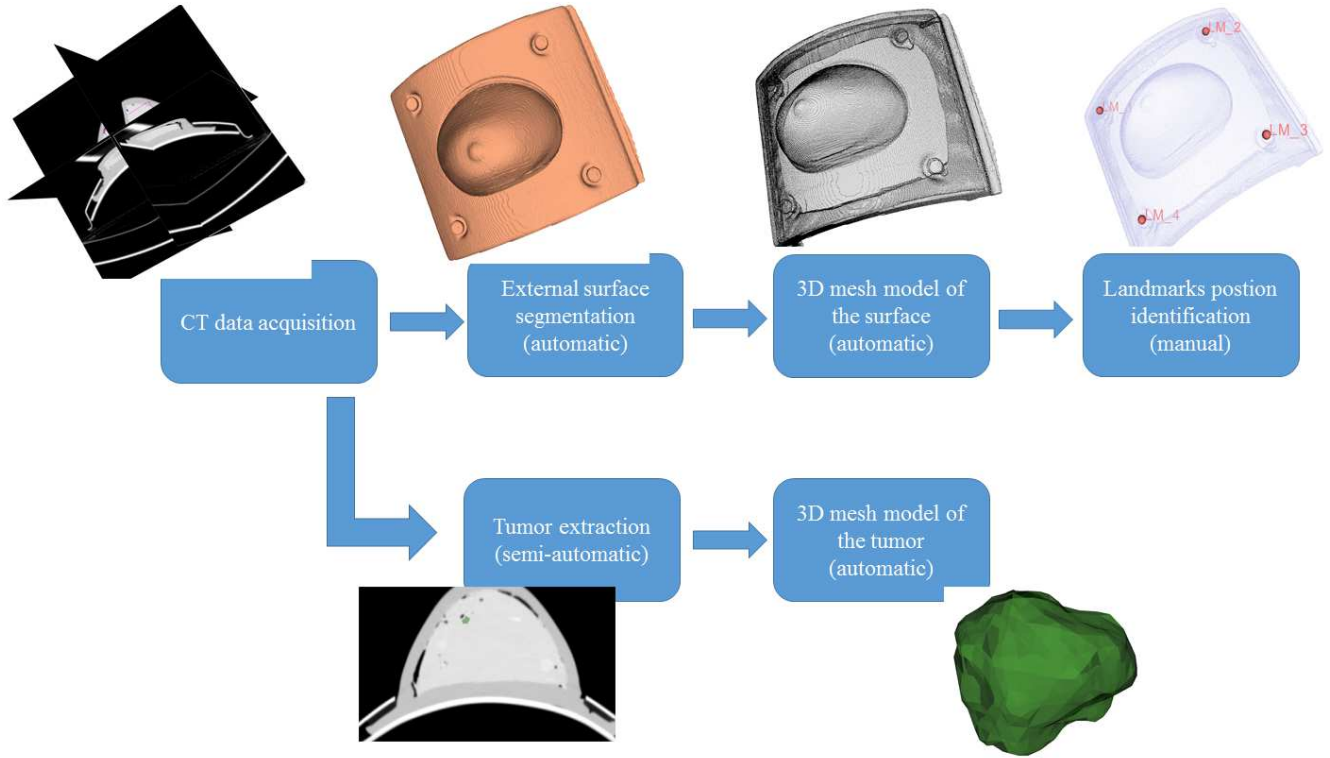


Figure 3. Overview of the image acquisition and processing workflow. From the CT data we segment the external surface of the breast, the tumors and the landmarks used for the rigid registration (section 3.1)

tation Toolkit ITK-SNAP software [20] from which a triangulated mesh is generated. The locations of the landmarks were manually determined and recorded (Figure 3).

3 Registration method

The scope of the registration method that we want to implement is to minimize the distance between a set of points that represents the surface of the phantom in the first position which is fixed, also called the reference position, and the points on the surface of the phantom in the second position which is moving, also called target position.

If we denote $T = \{T_i\}$ the set of points of the target surface and $R = \{R_i\}$ the set of points of the reference surface, the goal is to find a transformation f , $f = (f_1, f_2, f_3) : \mathbb{R}^3 \rightarrow \mathbb{R}^3$ such that:

$$\sum_i \|f(T_i) - R_i\|^2 = \min. \quad (1)$$

In the case of the rigid registration, one of the most used methods, called iterative closest point (ICP), was first introduced by Besl and McKay in [3]. The ICP method alternates between the computation of the rigid transformation and the determination of the correspondences, while in our case we solve the rigid registration by using markers on the base of the phantom in order to get the correct correspondences after.

The entirety of our registration approach is captured in Figure 4. Briefly described, an initial rigid alignment is performed using the landmarks identified after the acquisition (section 2). The landmarks are the four black screws located on the rigid base of the phantom (figure 1). Once complete, we identify the best correspondences on the two rigidly aligned surfaces as we describe in the section 3.2. The correspondences will drive the computation of the TPS coefficients that will completely parametrize the registration transformation f . The combined rigid and nonrigid transformations provides a mean to map the tumors identified in the reference dataset with the tumors identified in the target dataset.

3.1 Rigid alignment

An initial rigid alignment is performed using the landmarks located on the breast support (Figure 3). The registration of corresponding landmarks uses a traditional 3D point-based singular value decomposition algorithm [1]. The point-based registration algorithm finds the optimal rotation matrix A and translation vector v to minimize the fiducial registration error as defined by equation (1) using only a subset $\{LM\} \subset \{T_i\}$ and $\{LM'\} \subset \{R_i\}$ represented by the segmented landmarks (Figure 4).

In this case $f(LM) = ALM' + v$

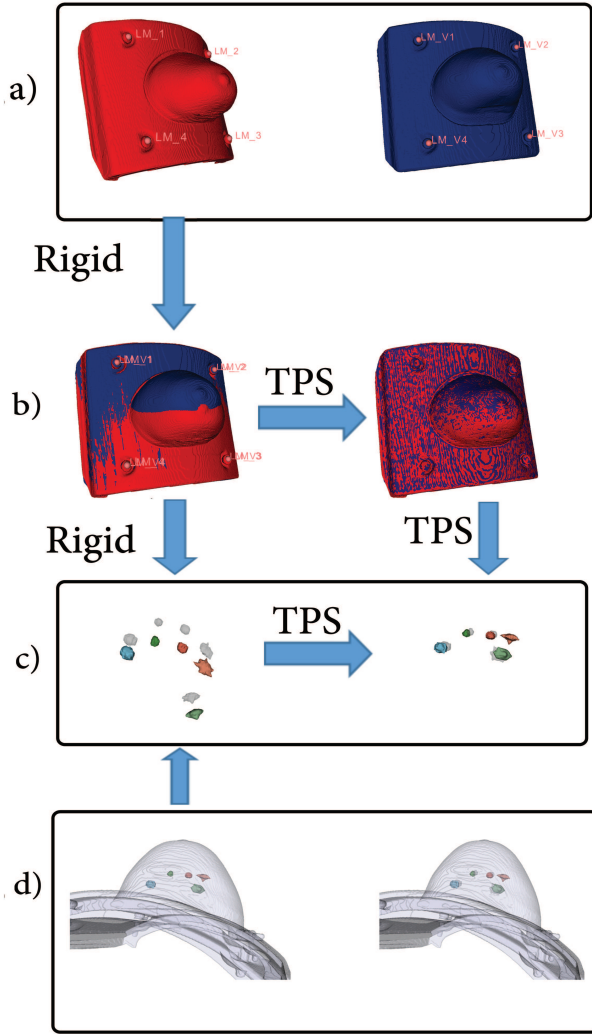


Figure 4. a) Reference(left) and target (right) datasets with four landmarks highlighted in the corners. b) Rigid registration (left) and TPS registration(right) results c) Rigid registration applied to the tumors (left) followed by the nonrigid TPS deformation(right). The reference tumors are colored while the target tumors are grey. d) The reference and target surfaces with tumors inside.

3.2 Correspondences and TPS surface registration

The second step, once we have the rigid alignment, is to compute the correspondences between each of the points in the target dataset with points belonging to the reference dataset.

The deformation between the different acquisitions is due to the gravitational force, therefore the first option is to project along the direction of the gravity the target points to the reference surface to get the closest point. Another option is to compute the closest point on the reference surface for each point of the target surface using the euclidean distance. We have obtained similar results employing both methods. By using these methods to compute the corre-

spondences, we ensure the preservation of the topology of the target surface.

Once the correspondences are computed, the TPS interpolation is given by:

$$f_i(x) = \sum_j c_j^i \rho(\|x - R_j\|) + \langle z^i, x \rangle, \quad (2)$$

where z^i is a 1×4 matrix representing a row of the affine transformation $z = [z^1; z^2; z^3]$, $c = \{c_j^i\}$ is a warping coefficient matrix representing the non-affine deformation and $\rho(r) = r$ represent the kernel function in the 3D case. $\langle z^i, x \rangle$ is the scalar product using the homogeneous representation of the argument x as follows:

$$\langle z^i, x \rangle = z_0^i + z_1^i x_1 + z_2^i x_2 + z_3^i x_3 \quad (3)$$

The TPS function not only fulfill the minimization condition (1) but minimize also the bending energy or the smoothness measure given by the integral of the square of the second derivative [19]:

$$\mathcal{S}(f) = \sum_{j=1}^3 \int \sum_{m,n=1}^3 \left(\frac{\partial^2 f_j}{\partial x_m \partial x_n} \right)^2 dx_1 dx_2 dx_3, \quad (4)$$

It is not difficult to prove, see [13] or [19], that c can be obtained by solving the following system of linear equations:

$$\begin{pmatrix} P & B \\ B^T & 0 \end{pmatrix} \begin{pmatrix} c \\ z^T \end{pmatrix} = \begin{pmatrix} T \\ 0 \end{pmatrix} \quad (5)$$

where $P_{j,k} = \rho(\|R_j - R_k\|)$, and $B = (1; R)$.

Beside the fact that it minimizes the bending energy there are two advantages that led us to use TPS:

- it can be decomposed into a linear part, given by the matrix z and a non-linear deformation, given by the matrix c
- its solution is obtained in closed form (see equation (5)).

4 Registration results

The proposed registration method was evaluated on 5 previously segmented tumors in each of the four positions of the phantom. We are interested to know how well a registration method based only on the external surface information may solve for the internal structures such as the tumors. First, we apply the rigid registration obtained from the alignment of the landmarks, then the non rigid TPS function (equation (2)) obtained from the surface registration is applied to each of the points x of the target tumor. We also keep into account the triangulation of the tumor mesh before and after the registration in order to assess the consistency of topological structure. This check is important as there are other methods that may non-rigidly align two sets of points

Tumor number		Rigid registration error (mm)	TPS registration error (mm)
1	Mean	11.82	4.09
	Std. dev.	3.41	2.19
	Minimum	5.59	2.03
	Maximum	14.96	6.34
2	Mean	14.09	4.86
	Std. dev.	4.39	1.98
	Minimum	6.51	2.24
	Maximum	17.75	6.52
3	Mean	14.27	5.34
	Std. dev.	3.97	2.23
	Minimum	6.45	1.99
	Maximum	18.63	6.08
4	Mean	11.84	4.95
	Std. dev.	3.53	2.62
	Minimum	5.49	1.57
	Maximum	15.03	5.49
5	Mean	13.63	5.14
	Std. dev.	4.29	2.24
	Minimum	6.40	2.07
	Maximum	19.04	6.17
Global	Mean	13.13	4.71
	Std. dev.	3.80	2.45
	Minimum	5.59	2.03
	Maximum	19.04	6.52

Table 1. Registration results

(e.g. [14]) but their success is based on the morphing of one structure into the other without maintaining the topology of the underlying meshes. We tried these methods as well, however, we have not achieved desired results.

An illustration of the result of the application of TPS registration to the tumors inside the phantom is given in the row c) of the Figure 4. The numeric results can be found in the Table 1. The error from the rigid landmarks registration was evaluated on the landmarks center at around 0.5 mm, while the error evaluated on the centroid of the tumor volume was around 5mm (last column in the table).

In a relatively recent work, [9], a complex model for breast deformation prediction using patient-specific biomechanical models obtained the same accuracy of about 5 mm when computed as the euclidean distance between landmarks previously segmented at specific locations, therefore our results prove that even with a very simple and efficient solution we can achieve comparable results.

5 Conclusions and future works

We have introduced here a preliminary study for breast registration to be used in an image guided biopsy procedure. The use of the phantom allowed us to have the complete control of the registration error, therefore to assess the goodness of the method in an objective way. We have obtained

an accuracy below 5mm which is compatible with the clinical requirements for a tumor with the diameter of more than 10mm.

The registration procedure includes rigid and nonrigid methods and was tested on a realistic breast phantom that underwent deformation due to the gravitational force. By computing the point to point correspondences of the rigidly aligned surfaces and subsequently deriving the TPS parameters, we have found the registration solution in closed form. The computational time is compatible with the real-time requirement since, beside the rigid tracking which can be easily implemented in real-time using available technologies such as optical trackers and markers, the TPS solution involves the resolution of a linear system of equations. From the experiments, we deduced that the shifts and the deformations of the tumors were very accurately solved nearby the surface but not so accurately when the tumors lies toward the center of the breast. In fact, the TPS model is based on the displacement of the control points which, in our case, lie on the breast surface.

To our knowledge, there are no image guided breast biopsy systems that include the registration of different positions of the breast, therefore these results are very encouraging at this early stage and many avenues for future works are possible. New methods for the computation of the unknown correspondences (e.g. [11]) will be implemented in future works.

Certainly, the first expansion of this work will include a test on patients. The main differences with the proposed system will lie into the image acquisition and processing. We envision to use a surface scanner for the breast surface acquisition, an optical tracker for the landmark localization and an ultrasound machine for the intraoperative lesion localization. The system shall include a step for the registration of the intraoperative surface with the preoperative radiologic images.

6 Acknowledgements

The work described in this paper has received funding from the European Union's Horizon 2020 Research and Innovation programme under Grant Agreement no. 688188 as part of the MURAB (MRI and Ultrasound Robotic Assisted Biopsy) project.

References

- [1] Arun, K.S., Huang, T.S., Blostein, S.D.: Least-squares fitting of two 3-d point sets. *IEEE Transactions on Pattern Analysis and Machine Intelligence* 9(5), 698–700 (1987)
- [2] Behrenbruch, C.P., Marias, K., Armitage, P.A., Yam, M., Moore, N., English, R.E., Clarke, J., Brady, M.: Fusion of contrast-enhanced breast mr and mammographic imaging data. *Medical Image Analysis* 7(3), 311–340 (2003)

- [3] Besl, P.J., McKay, N.D.: Method for registration of 3-d shapes. In: Robotics-DL tentative, pp. 586–606. International Society for Optics and Photonics (1992)
- [4] Boehler, T., Zoehrer, F., Harz, M., Hahn, H.K.: Breast image registration and deformation modeling. *Critical Reviews in Biomedical Engineering* **40**(3) (2012)
- [5] Bookstein, F.L.: Principal warps: thin-plate splines and the decomposition of deformations. *IEEE Transactions on Pattern Analysis and Machine Intelligence* **11**(6), 567–585 (1989)
- [6] Carter, T.J., Sermesant, M., Cash, D.M., Barratt, D.C., Tanner, C., Hawkes, D.J.: Application of soft tissue modelling to image-guided surgery. *Medical engineering & physics* **27**(10), 893–909 (2005)
- [7] Causer, P.A., Piron, C.A., Jong, R.A., Plewes, D.B.: Preliminary in vivo validation of a dedicated breast MRI and sonographic coregistration imaging system. *American Journal of Roentgenology* **191**(4), 1203–1207 (2008)
- [8] Conley, R.H., Meszoely, I.M., Weis, J.A., Pfeiffer, T.S., Arlinghaus, L.R., Yankeelov, T.E., Miga, M.I.: Realization of a biomechanical model-assisted image guidance system for breast cancer surgery using supine mri. *International journal of computer assisted radiology and surgery* **10**(12), 1985–1996 (2015)
- [9] Han, L., Hipwell, J.H., Tanner, C., Taylor, Z., Mertzaniidou, T., Cardoso, J., Ourselin, S., Hawkes, D.J.: Development of patient-specific biomechanical models for predicting large breast deformation. *Physics in Medicine and Biology* **57**(2), 455 (2011)
- [10] Hipwell, J.H., Vavourakis, V., Han, L., Mertzaniidou, T., Eiben, B., Hawkes, D.J.: A review of biomechanically informed breast image registration. *Physics in medicine and biology* **61**(2), R1 (2016)
- [11] Maris, B.M., Fiorini, P.: Generalized shapes and point sets correspondence and registration. *Journal of Mathematical Imaging and Vision* **52**(2), 218–233 (2015)
- [12] Maris, B.M., Fiorini, P.: Retrospective Study on Phantom for the Application of Medical Image Registration in the Operating Room Scenario. *Proceeding (832) Biomedical Engineering - 2016* (2016). DOI 10.2316/P.2016.832-029
- [13] Modersitzki, J.: FAIR: Flexible Algorithms for Image Registration. SIAM, Philadelphia (2009)
- [14] Myronenko, A., Song, X.S.X.: Point Set Registration: Coherent Point Drift. *IEEE Transactions on Pattern Analysis and Machine Intelligence* **32**(12), 2262–75 (2010)
- [15] Ong, R.E., Ou, J.J., Miga, M.I.: Non-rigid registration of breast surfaces using the laplace and diffusion equations. *Biomedical engineering online* **9**(1), 1 (2010)
- [16] Piron, C., Causer, P., Jong, R., Shumak, R., Plewes, D.B.: A hybrid breast biopsy system combining ultrasound and mri. *IEEE transactions on medical imaging* **22**(9), 1100–1110 (2003)
- [17] Pleijhuis, R.G., Graafland, M., de Vries, J., Bart, J., de Jong, J.S., van Dam, G.M.: Obtaining adequate surgical margins in breast-conserving therapy for patients with early-stage breast cancer: current modalities and future directions. *Annals of Surgical Oncology* **16**(10), 2717–2730 (2009)
- [18] Rueckert, D., Sonoda, L.I., Hayes, C., Hill, D.L., Leach, M.O., Hawkes, D.J.: Nonrigid registration using free-form deformations: application to breast MR images. *IEEE Transactions on Medical Imaging* **18**(8), 712–21 (1999)
- [19] Wahba, G.: *Spline Models for Observational Data, CBMS-NSF Regional Conference Series in Applied Mathematics*, vol. 59. SIAM (1990)
- [20] Yushkevich, P.A., Piven, J., Hazlett, H.C., Smith, R.G., Ho, S., Gee, J.C., Gerig, G.: User-guided 3d active contour segmentation of anatomical structures: significantly improved efficiency and reliability. *Neuroimage* **31**(3), 1116–1128 (2006)